



Supporting Online Material for

Cortex is Driven by Weak but Synchronously Active Thalamocortical Synapses

Randy M. Bruno* and Bert Sakmann

*To whom correspondence should be addressed. E-mail:
bruno@mpimf-heidelberg.mpg.de

Published 16 June 2006, *Science* **312**, 1622 (2006).
DOI: 10.1126/science.1124593

This PDF file includes

Materials and Methods
SOM Text
Figs. S1 to S7
References

SUPPORTING ONLINE MATERIAL

MATERIALS AND METHODS

Surgery

Thirty-five Wistar rats (P24-35, mean P29, 65-145 g, Charles River) were maintained in either a lightly-sedated state using fentanyl ($n = 28$) or an anesthetized state using urethane (1.6 g/kg given intraperitoneally; 10% supplements given as necessary; $n = 7$). The urethane preparation produces deep anesthesia corresponding to a stage III-4 anesthetic depth (*S1*). The fentanyl preparation does not produce deep anesthesia but rather light sedation and analgesia and is more similar to stage III-1 depth (see below “Effects of Fentanyl”).

In both preparations, body temperature was maintained at 37°C by a servo-controlled heating blanket. A metal post for positioning the head was attached to the skull overlying the cerebellum by dental acrylic. Screws were inserted in the right frontal and occipital bones for electrocorticogram recording. Craniectomies were made overlying left barrel cortex (each $<0.5 \text{ mm}^2$) and VPM of the thalamus ($<2.0 \text{ mm}^2$). The VPM craniectomy was centered at 3.5 mm posterior to bregma and 3.0 mm lateral of the midline.

The sedated preparation has been described previously (*S2*). Briefly, surgeries for this preparation were performed under isoflurane. The right jugular vein was cannulated for intravenous drug infusion, the left femoral artery cannulated for blood pressure monitoring, and a tracheotomy was performed. For neural recordings, isoflurane was discontinued, and the rat was maintained in a lightly narcotized state by intravenous infusion of fentanyl ($\sim 10 \mu\text{g} / \text{kg} / \text{hr}$). To prevent spontaneous whisker movement, neuromuscular blockade was induced with pancuronium bromide (1.6 mg / kg / hr), and the animal artificially respired (~ 90 breaths/min) using a positive-pressure ventilator. A computer continuously monitored electrocorticogram, mean arterial pressure, arterial pulse rate, and tracheal airway pressure. Experiments were terminated if any of these indicators could not be maintained within normal physiological range. Experiments typically lasted 16-20 hours.

Electrophysiology

Extracellular recordings were made from VPM as previously described (S3) using quartz-insulated platinum and 10% tungsten core electrodes (5-10 M Ω impedance). In later experiments, loose-seal cell-attached recordings were made with glass pipettes (ID < 1 μ m) filled with artificial cerebrospinal fluid (in mM: 135 NaCl, 5.4 KCl, 1.8 CaCl₂, 1.0 MgCl₂, and 50 HEPES; pH 7.2). Electrodes were advanced slowly along the dorsal-ventral axis. Signals were amplified, bandpass-filtered 0.3–9 kHz, and acquired at 32 kHz using custom software implemented in LabView v7.

We searched for TC units during manual or ramp-and-hold whisker deflection (see below). APs were recorded only when at least three times larger than background noise. Typically, signal:noise ratios were on the order of 10:1, and recordings consisted of only a single positive-going unit. Spike-sorting was used to check the quality of single-unit isolation (S3).

Patch pipettes were pulled from unfilamented borosilicate glass using a 3- or 4-stage pull. The outside diameter of the shank entering the brain was < 75 μ m. Pipettes were tip-filled with (in mM) 135 K-gluconate, 10 HEPES, 10 phosphocreatin-Na, 4 KCl, 4 ATP-Mg, 0.3 guanosine triphosphate, and 0.2% biocytin (pH 7.2, osmolarity 291). Internal solutions were kept on ice during experiments. Patch pipettes were inserted perpendicular to the pia, and cells were searched for blindly (S4). Recordings were made in Bridge mode and digitized at 32 kHz. Seal resistance was > 1 G Ω , access resistance 1-100M Ω , and spike height and overall V_m were stable throughout the recording. No holding current was used. Pipette capacitance was neutralized prior to break in. To prevent crosstalk, thalamic and cortical A/D converter channels were separated by a channel fitted with a grounding lug. A ground shield was placed directly between the electrodes.

Whisker Stimulation

Individual whiskers were deflected using multi-directional piezoelectric stimulators (S5). A stimulator was attached to a whisker ~5 mm from the base of the hair, which was deflected 5.7° (500- μ m amplitude) using relatively high-velocity (onset and offset: ~570° / sec) ramp-and-hold movements (S2). The whisker was held deflected for a 200-ms period between stimulus onset and offset. Deflection amplitude was calibrated using a

microscope, and possible ringing of stimulators was ruled out using a fiber optic displacement sensor. Deflections were applied randomly in each of eight directions, in 45° increments relative to the horizontal alignment of the rows. The whisker that elicited the strongest PSP response was deemed the PW. A receptive field was mapped by applying twenty blocks of such stimuli to the PW (160 total stimuli).

To obtain a large number of thalamic trigger events for spike-triggered averaging, we applied a 1- or 2-Hz sinusoidal stimulus with an amplitude of 5.7° to the PW for 2 sec. The sinusoid was applied in the angle that evoked the most APs from the thalamic neuron during ramp-and-hold deflections. Typically we ran 100-400 trials (2-3 sec interstimulus intervals). The sinusoidal stimuli have relatively low mean velocity (e.g., ~22.8° / sec for a 2-Hz sinusoid) and evoke a substantial number of thalamic APs, like the ramp-and-hold stimulus, but disperse them over hundreds of msec throughout a cycle as can be seen from the population PSTH (Fig. S2A). In contrast, thalamic APs are concentrated into a 25-ms period during the higher-velocity ramp-and-hold stimulus (Fig. S2B).

Average Post-Synaptic Potential Estimation

Neuronal recordings were checked for stationarity by plotting, by trial, the total number of thalamic APs and the mean cortical V_m . Only data in which neither cell showed any overall increase/decrease was analyzed.

Prior to averaging, cortical APs must be removed from whole-cell records so as to not confound measurement of TC synapse-evoked EPSPs with APs generated at the axon hillock. APs were removed from V_m traces by thresholding to determine AP times and replacing 200-800 μ s before the AP peak and 1-3 ms after with an interpolated straight line. All APs were screened visually, and the pre- and post-peak parameters set manually for each cell so as to remove just the AP and the after-hyperpolarization (Fig. S3A). This method affected less of the V_m record than other methods we tested such as median filtering (S6), which is sensitive to the choice of filter size and the variability of AP duration. The AP timescale (1-4 ms) is an order of magnitude smaller than the EPSP timescale (~20-30 ms), and the AP firing rates of excitatory cortical neurons are relatively low during the sinusoid (Fig. 1A, Figs. S3A and S5, A & C) and even during the more effective ramp-and-hold stimulus (Fig. 4F, Fig. S4C). Thus, interpolated regions

account for an extremely small portion of the data. The APs that they replace are two orders of magnitude larger than the EPSPs to be measured and would skew aPSPs if they were not filtered out.

Whether a connection between the cells exists or not, cortical V_m will co-vary with the thalamic APs over the timescale of a stimulus. This is because the thalamic and cortical cells are both part of the network that is activated by movement of that particular whisker. The net activity of all the thalamic inputs under these conditions is stimulus-locked, and their relative synchrony has been thought to be a function of stimulus parameters in the whisker (S7, S8) and the visual system (S9). Our data directly demonstrate this notion (see “Stimuli Effects on Thalamic Synchrony” below). We collected a large number of thalamic APs while holding thalamic synchrony at a low level by applying a weak sinusoidal deflection to the principal whisker.

Cortical V_m was averaged around the time of individual thalamic APs collected during deflection (Fig. S3B, left panel). The average contribution of non-recorded inputs to V_m can thus be estimated by shifting the records of V_m by one trial and computing a new average (Fig. S3B, middle panel). If a synaptic connection exists between a pair of cells, the difference of these two averages should estimate the average unitary EPSP evoked in the cortical cell by the thalamic neuron (Fig. S3B, right panel). The timescale of this potential change is orders of magnitude faster than the timescale of the stimulus (tens of milliseconds vs. hundreds of milliseconds to seconds), indicating that the change is not an artifact of the stimulus.

The shift corrector can have a variety of shapes (compare Figs. 1B and Fig. S5D). Its shape should mainly be determined by the profile of the individual thalamic PSTH and the average of cortical V_m with regard to the stimulus. These two response functions do not necessarily smoothly follow the sinusoidal stimulus in all cases. Often they each respond to one or more phases of the sinusoid, and these phases may or may not overlap. The response functions thus contain higher frequencies than the sinusoid itself, and can produce baselines with higher frequencies than the sinusoid.

From the subtraction, the mean V_m during the 20-ms period preceding the thalamic discharge was calculated and used to set a 99% significance limit from V_m at 1 msec after

the thalamic AP. Fluctuations crossing this limit during the +1 to +5 ms interval were deemed statistically significant.

Although our procedure estimates and subtracts off the contributions of unrecorded thalamic inputs and cortical inputs triggered by them, possible influence of a polysynaptic pathway between the recorded thalamic and cortical neuron cannot be completely ruled out. Such pathways are, however, unlikely to influence the aPSP because each synapse in the chain has only a small probability of evoking an AP in the next cell, and the product of multiple small probabilities quickly converges to near 0 values.

The polysynaptic routes having the greatest chance of influencing the aPSP amplitude are disynaptic excitation and inhibition evoked by the recorded thalamic neuron. We consider disynaptic inhibition, thought to be stronger in this system (*S10, S11*). A thalamic neuron does not contact all of the inhibitory neurons in the aligned barrel (*S3*). Where a TC-inhibitory neuron contact is made, a thalamic AP has only a 1 in 20 chance of evoking a spike in the post-synaptic neuron, and then with up to 20 ms of jitter (*S3*). Thus, the thalamic AP has roughly only a 1 in 100 chance of evoking in a contacted inhibitory interneuron a spike early enough to affect the rising phase of the aPSP. The probability of an arbitrary inhibitory cell contacting an arbitrary excitatory neuron in the same barrel is not known, but the percentage found to be connected *in vitro*, given selection criteria, is between 20 and 50% (*S11, S12*). Thus, the final chances of the recorded thalamic neuron itself directly evoking a reliable short-latency disynaptic inhibitory PSP onto the recorded cortical cell is low enough to have negligible consequences for aPSP amplitude measurements. The impact of such IPSPs may of course be more significant for the later decaying phase of the aPSP.

Burst-Triggered Averaging

Low-threshold calcium bursts in thalamic cells (*S13*) were evoked electrically by juxtасomally applying 5-20 nA of hyperpolarizing current for 10-40 msec through the recording pipette. Burst-triggered averages were calculated by averaging cortical V_m around the time of the first AP in the burst.

Histology

The rat was deeply anesthetized with ketamine and perfused transcardially with phosphate buffer followed by 4% paraformaldehyde. Cortex and thalamus were cut tangentially and coronally, respectively, in 100- μ m vibratome sections and stained for cytochrome oxidase (CO) and biocytin (*S14*). Well-filled cells were reconstructed using a NeuroLucida system with a 100X/1.4NA oil-immersion objective. The barrel field was reconstructed on the basis of the CO staining.

An L4 neuron was classified as barrel or septa depending on whether or not the soma was in a CO-rich area. Because tangential sections are usually not perfectly tangential to the pia, superficial layer 2/3 cells cannot always be reliably assigned to the more deeply located barrels on the basis of a camera lucida reconstruction. We therefore confirmed the barrel column identity of a layer 2/3 cell by tracing its main axon trunk into layer 4 (*S15*). Thalamic recording sites were confirmed by an electrolytic lesion through the thalamic metal electrode at the end of the experiment, or including 0.2% biocytin in the thalamic pipette and filling the cell juxtасomally (*S16*).

Data Analysis

Data was analyzed using Excel and custom-written Matlab routines. All statistical comparisons are non-parametric two-tailed tests unless otherwise noted. Means \pm SEM are given throughout except where otherwise noted.

SOM Text

EFFECTS OF FENTANYL

The fentanyl preparation was used to record activity in a lightly-sedated state, which by a number of measures is a better proxy for normal physiology than the anesthetized preparation is. Unparalyzed animals, given the dosage of fentanyl used here, have been reported to exhibit tranquilized behavior but still make spontaneous movements (*S2*). In our hands, mean arterial blood pressure ranges from 100-130 mm Hg during sedation, similar to healthy awake rats. During sedation, VPM spontaneous activity (median 5.4 Hz) and receptive field size are similar to previous reports of firing rates in awake animals (*S17*). V_m of L4 neurons during sedation is also similar to that of the awake animal (Fig. S5, A & C, also Bruno & Sakmann, in preparation). It has previously been

reported that sensory-evoked responses of L4 barrel neurons recorded extracellularly are not obviously different between sedation and wakefulness (*S18*). Finally, other than an expected slight increase in spindle-like activity during sedation, we observed no differences between the EEG recordings of our sedated and awake animals. In contrast to these two states, we observed in urethane-anesthetized animals, as partially reported by others (*S1*), suppressed blood pressure, decreased thalamic discharge and receptive field size, UP/DOWN oscillations in cortical V_m , and distinctly different EEG patterns.

The narcotic fentanyl is a mu-opioid receptor agonist similar to morphine. Mu-opioid receptors are sparsest in primary sensory areas, being most densely concentrated in the limbic and frontal areas (*S19*, *S20*), which along with peripheral and subcortical regions are thought to mediate its analgesic and sedative effects. Particularly sparse levels are observed in L4 of granular areas of somatosensory cortex, such as barrel cortex, where most of the detectable signal resides instead in layers 1 and 5A (*S19*, *S20*). This pattern of labelling corresponds to the projection from the second-order somatosensory (posterior medial) nucleus rather than the VPM projection (*S20*). Therefore, the low dose of fentanyl used here is itself unlikely to depress the efficacy of the VPM-layer 4 synapse.

To test directly whether or not fentanyl at this dosage affects aPSP amplitude, we recorded the same connected pairs under both unsedated and sedated conditions ($n = 2$ pairs). To achieve this, the sedated preparation was modified as follows. At the end of the initial surgery, wounds were infiltrated with 0.25% bupivacaine, a long-lasting local anesthetic. As the animal was transferred to the ventilator, paralytic was administered intravenously without fentanyl, and isoflurane gas (1-2%) was delivered via the ventilator to continue general anesthesia. Preliminary mapping of thalamus and cortex and isolation of a single VPM neuron were performed under anesthesia.

Prior to patching the cortical neuron, isoflurane was discontinued. In our hands and those of others, animals wake up rapidly from isoflurane (after 2-5 min). After a period of 10-15 min, we established a whole-cell recording from an aligned cortical neuron. The aPSP of this unsedated condition was then estimated by collecting 100-200 trials of data during the sinusoidal whisker stimulus. A loading bolus of fentanyl (~10 $\mu\text{g}/\text{kg}$) was then injected intravenously over a period of several minutes. Dead space in the tubing had

been measured prior to the experiment and was corrected for during the injection. The EEG showed a small increase in the frequency of spindle-like activity confirming that the drug was properly administered. Additional fentanyl was continuously infused at our usual flow rate. After an additional 10-min period had elapsed, the aPSP estimation procedure was repeated.

Fig. S5 shows a connected pair under both awake and sedated conditions. There was no obvious difference between the conditions in terms of spontaneous or evoked activity in the thalamus or cortex (Fig. S5, A & C). APSPs were estimated for the pair pre- and post-drug (Fig. S5, B & D). An overlay of pre and post aPSPs, aligned by the baseline value at their onsets, shows no difference in risetime or amplitude (Fig. S5E). There may be a change in aPSP decay, but such slow timescale changes are difficult to judge as they are more easily influenced by slow-wave fluctuations in the baseline. We repeated this experiment in a second pair, which also showed no change of aPSP amplitude (pre 826 μV , post 799 μV). We conclude that this dosage of fentanyl does not strongly suppress VPM-layer 4 efficacy and is not an explanation for the small size of the connection strengths we observed.

STIMULI EFFECTS ON THALAMIC SYNCHRONY

The degrees to which different stimuli synchronized thalamic neurons were directly measured by simultaneous extracellular recordings of multiple VPM neurons, recorded either on the same electrode or separate electrodes in the same barreloid. To be included in analyses, pairs recorded on the same electrode had to have waveforms that were distinctly different (i.e., producing non-overlapping clusters during off-line spike sorting) (S3). Usually one waveform was initially positive-going, and the other negative-going. Cross-correlation histograms (correlograms) were made separately for spontaneous and stimulation periods (Fig. S6). For any given condition, we found no differences between correlograms having binwidths of 0.1, 0.5, 1.0 and 2.0 ms other than small binwidths leading to correlograms with more noise. A binwidth of 1.0 ms was therefore used for these analyses, producing a reasonable tradeoff between noise and resolution.

Some pairs of thalamic neurons showed synchrony during periods of spontaneous activity, such as in Fig. S6, A & B, left. The sinusoidal stimulus used to increase thalamic

firing rates during aPSP estimation did not noticeably increase their synchrony (Fig. S6, A & B, middle). We quantified how many near-synchronous events occur on the timescale of an EPSP, using a simple measure that normalizes for the firing rates of the two neurons (*S21*):

$$\text{strength} = \frac{N_c}{\sqrt{(N_1^2 + N_2^2)/2}}$$

where N_c is the sum of correlated events above baseline in a desired synchrony window, N_1 and N_2 are the numbers of cell 1 and 2 spikes used to compute the correlogram. We tested synchrony windows of ± 10 , 15, 20, and 25 ms, and results were similar in all cases. In the presented analyses, ± 20 ms was chosen, being similar to the EPSP timecourse. Baseline was taken to be the mean number of events at lags outside the timescale of an EPSP, namely for correlogram bins from ± 50 ms to within 5 ms of the window (e.g., for a window of ± 20 ms, bins from -50 to -25 and from +25 to +50).

Most systems for acquiring extracellular APs, both hardware- and software-based, impose a short lockout after the continuous signal crosses some amplitude threshold. For a given electrode, there exists therefore a brief period during which a subsequent AP cannot be detected, which is 0.5 ms in our case. Therefore, for pairs recorded on the same electrode, bins spanning ± 0.5 ms were excluded from analysis. As shown below, this does not affect any of our results. Moreover, narrow peaks (total widths limited to < 1 ms) were not observed in any of our two-electrode correlograms.

We compared the synchrony of such thalamic pairs during sinusoidal stimulation with periods of spontaneous activity (Fig. S6C). Thalamic pairs were not more strongly synchronized by the low-velocity sinusoid than during spontaneous activity (paired t test, $P = 0.28$, $n = 19$). This contrasts strongly with the synchronizing effect of the high-velocity ramp-and-hold stimulus (see Text and Fig. 6). Furthermore, synchrony was no different between spontaneous and sinusoidal stimulation when pairs were analyzed separately as “same electrode” and “two electrode” groups ($P = 0.08$, $n = 13$ and $P = 0.7$, $n = 6$, respectively; Fig. S6C). The trend-level difference for the subset recorded on the same electrode reflects that some of values during sinusoidal stimulation were slightly

smaller than those during spontaneous activity. This is in fact the opposite of the relationship that would potentially confound aPSP estimation. All of these results indicate that the sinusoidal stimulus does not enhance the trial-by-trial synchrony of thalamic neurons and consequently does not distort the aPSP.

We further used these data to test whether or not the shift procedure employed by the aPSP estimation correctly reflects the stimulus-induced correlations of non-recorded inputs. Shift correctors were computed for each of the thalamic pairs. The shift corrector for the example in Fig. S7 closely matched the correlation structure of the raw cross-correlogram (Fig. S7, C & D). Subtraction of these two yields a difference with no significant correlations present at any time interval (Fig. S7, E & F). None of the recorded thalamic pairs exhibited any correlation during stimulation that could not be captured by the shift corrector.

SUPPLEMENTAL FIGURE LEGENDS

Fig. S1. On-going synaptic activity *in vivo* masks individual unitary EPSPs and prevents identification. **(A)** Whole-cell recording from a layer 4 cortical neuron (*black trace*) and AP times of a simultaneously recorded thalamic neuron (*blue lines*) during spontaneous activity. This pair was connected having an aPSP of $\sim 300 \mu\text{V}$ (shown in Fig. S5). **(B-E)**, Close-ups of regions marked in **A**. *Arrow in (B)* A fluctuation occurs at a latency such that it conceivably could be a unitary EPSP but cannot even be measured due to the large changes affected by other synaptic inputs. *Arrow in (C)* This fluctuation starts before the AP and therefore cannot be a unitary. *Arrow in (D)* A fluctuation starts only 500 Ps after the AP, earlier than known conduction delays, but may be summing with a subsequent unitary.

Fig. S2. Stimuli having different velocities evoke thalamic discharges having different degrees of temporal dispersion. **(A)** Population PSTH of thalamic neurons' responses to a 2-Hz sinusoidal deflection of their respective principal whiskers ($n = 40$ cells). **(B)** Population PSTH of the responses of the same cells to ramp-and-hold deflections.

Fig. S3. **(A)** Example of removing an AP from a cortical whole-cell recording. This sweep was taken during 2-Hz sinusoidal stimulation. The zoomed view (*lower trace*) shows the original record (*solid line*) and the interpolated line (*long dashes*). **(B)** Method

of detecting unitary connections. Intracellular membrane potential of a cortical neuron (*Ctx*) is recorded at the same time as action potentials from a thalamic neuron (*Thl*). Cortical membrane potential is averaged around the time of individual thalamic APs during 2-sec 2-Hz sinusoidal deflections of the principal whisker (*left column*). Synchronous activity of thalamic cells is removed by shifting records of one cell by a single trial, computing a second spike-triggered average, and subtracting this from the first (*middle*). The difference is the impact of the recorded thalamic neuron on the cortical cell (*right*).

Fig. S4. Sub- and supra-threshold cortical responses to whisker deflection. **(A)** Average sub-threshold post-synaptic potentials (*red*) and supra-threshold action potentials (*blue*) of a star pyramid barrel neuron evoked by deflection (*grey*) of its principal whisker (C4) in 8 different directions. **(B)** Polar plots, summarizing traces in **a**, show the amplitude of average sub-threshold responses (*upper panel*) and number of action potentials (*lower*) evoked by deflections in different directions. *Middle panel* depicts the layout of the facial whiskers with regard to polar plots. Principal whisker here is colored black. **(C)** Scatterplot of all cortical cells shows that the preferred direction evokes on average 3 times as many APs as the average direction (response quantified over 200 ms following stimulus onset).

Fig. S5. Fentanyl sedation does not change aPSP amplitude. **(A)** Simultaneous recordings of cortical V_m (*upper*) and thalamic spiking (*lower*) in an unsedated animal under local anesthesia. **(B)** Spike-triggered average, shift-corrector, and aPSP estimate for the thalamocortical pair shown in (A) (n thalamic APs = 4503). **(C)** Example recordings from the same cells shown in (A) in the presence of fentanyl. **(D)** aPSP estimation in the presence of fentanyl (n thalamic APs = 4193). **(E)** Overlays of aPSPs determined during unsedated (*solid*) and sedated (*dashed*) conditions.

Fig. S6. Sinusoidal whisker deflection does not induce additional synchrony. **(A)** Cross-correlations of 2 thalamic neurons recorded on the same electrode during spontaneous activity (*left*), sinusoidal stimulation (*middle*), and high-velocity whisker deflection (*right*). **(B)** Similar analysis of 2 thalamic neurons recorded on different electrodes in the same barreloid. **(C)** Thalamic synchrony is typically similar for any given cell during

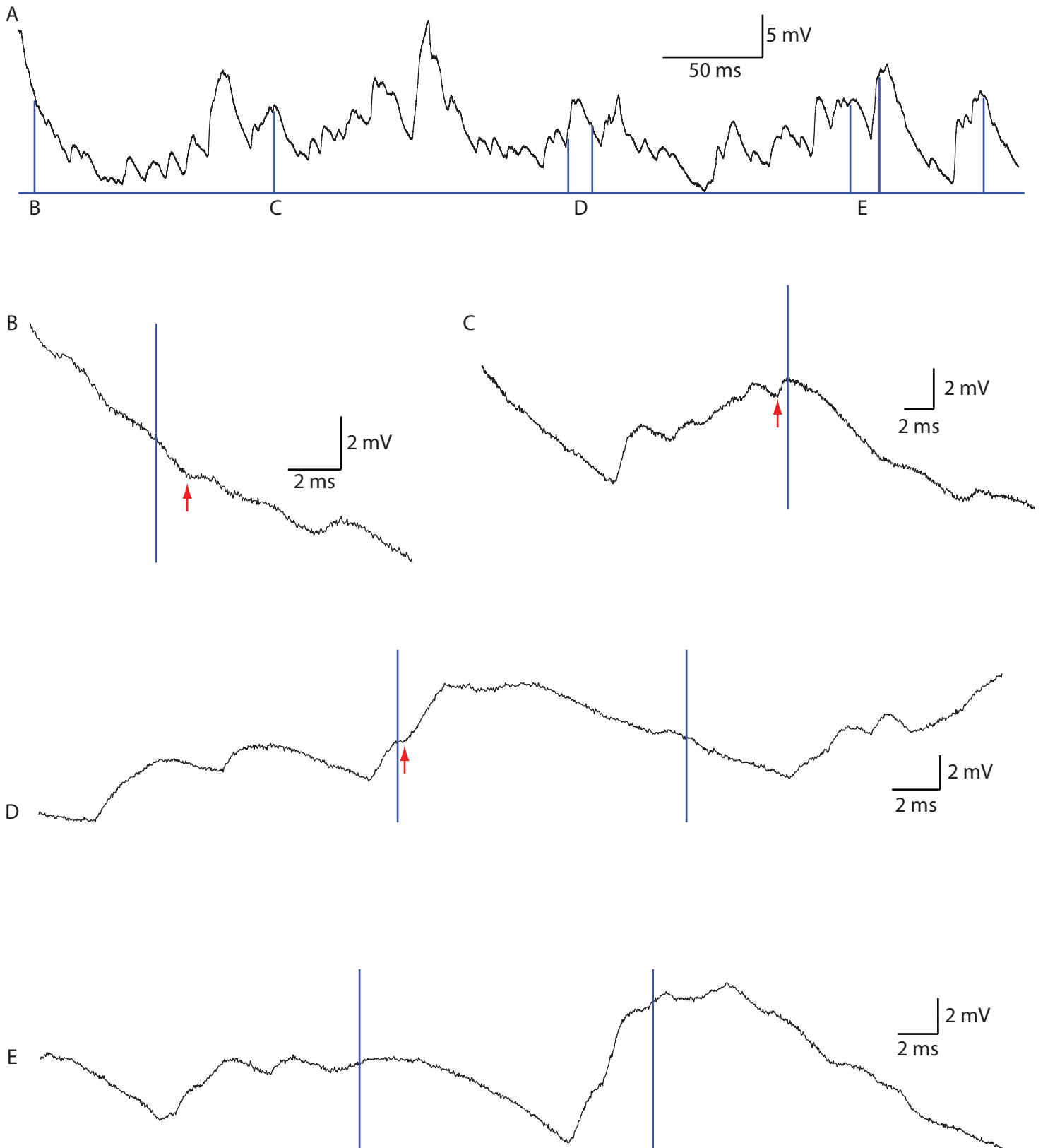
spontaneous activity and sinusoidal stimulation. *Line*, unity. *Circles*, thalamic pairs recorded on same electrode; *X's*, thalamic pairs recorded using 2 separate electrodes.

Fig. S7. Cross-correlation of pairs of simultaneously recorded thalamic neurons confirms that peripheral stimuli account for virtually relative correlations in thalamic firing during whisker deflection. **(A)** Schematic depicting experimental design. Two thalamic neurons in the same barreloid were simultaneously recorded on the same electrode. Sensory stimuli are able to synchronize these cells via diverging lemniscal afferents from brainstem. **(B)** AP trains from two simultaneously-recorded thalamic neurons during a 2-Hz sinusoidal whisker stimulus. **(C)** Cross-correlation histogram of the AP trains of the same thalamic pair collected over 400 trials ($n = 4464$ trigger spikes). **(D)** Synchronization due to the stimulus is estimated by shifting one of the thalamic trains by one trial and cross-correlating again. **(E)** Subtraction of C and D. Note that the corrected correlogram is essentially flat, indicating that after taking into account the effect of the stimulus the thalamic neurons fire independently of each other. **(F)** High-resolution (0.1-ms bins) corrected correlogram for lags spanning -50 to +50 ms.

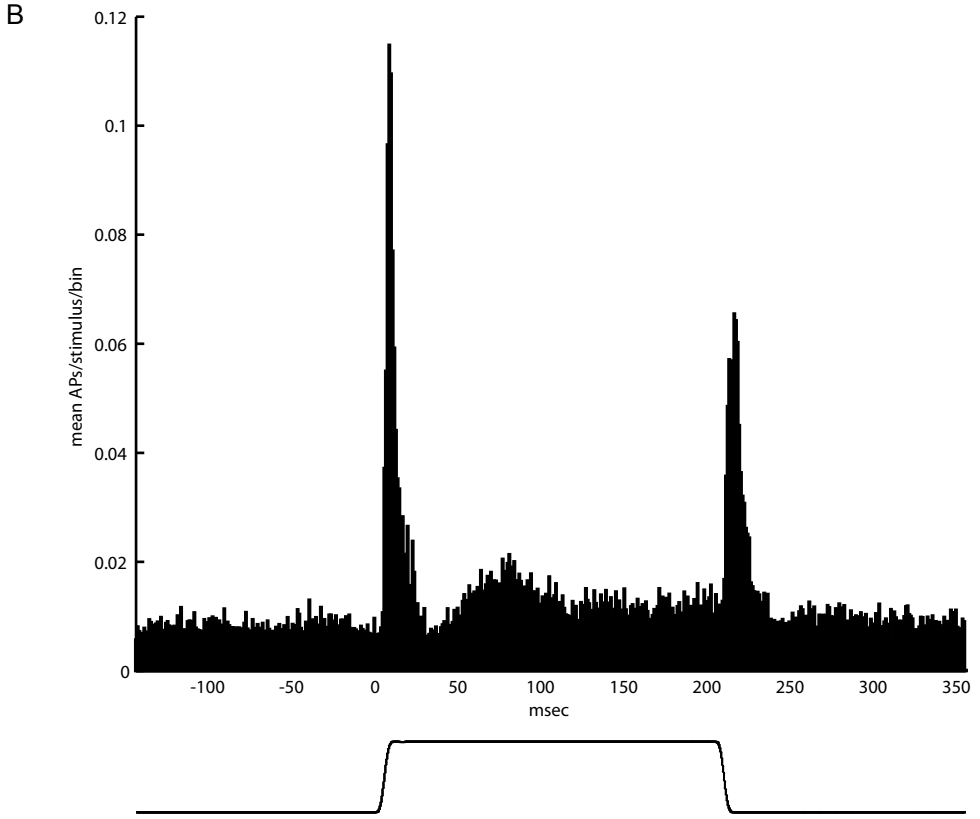
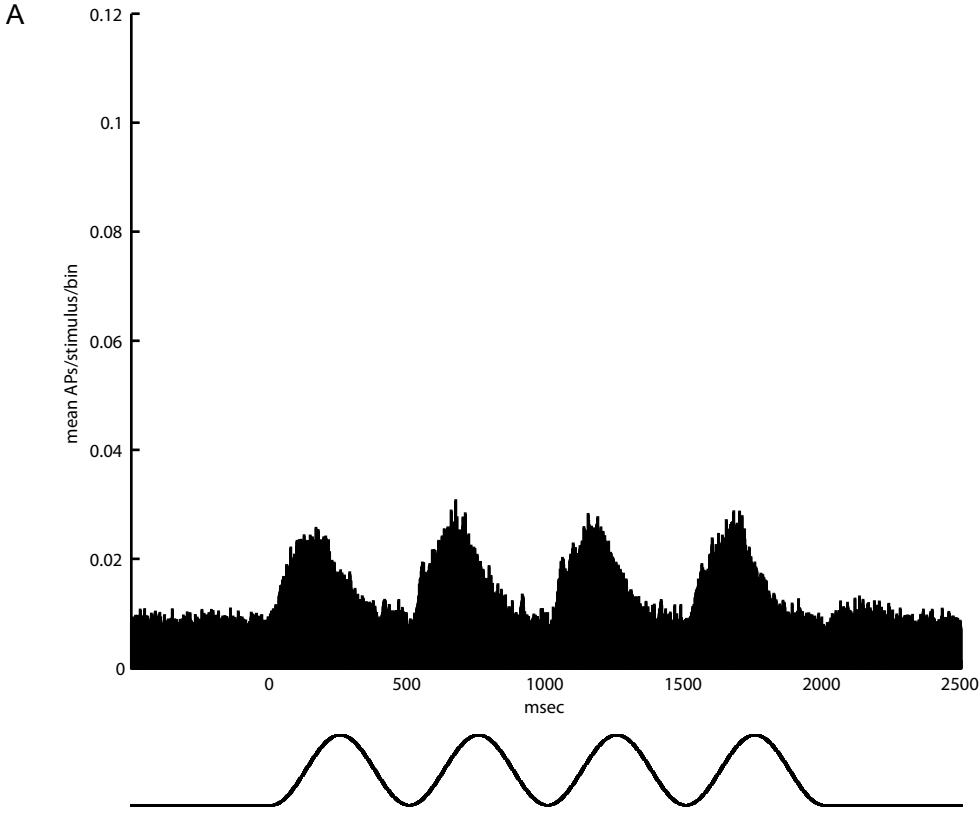
Supplemental References

- S1. M. H. Friedberg, S. M. Lee, F. F. Ebner, *J Neurophysiol* **81**, 2243 (1999).
- S2. D. J. Simons, G. E. Carvell, *J Neurophysiol* **61**, 311 (1989).
- S3. R. M. Bruno, D. J. Simons, *J Neurosci* **22**, 10966 (2002).
- S4. T. W. Margrie, M. Brecht, B. Sakmann, *Pflugers Arch* **444**, 491 (2002).
- S5. D. J. Simons, *Brain Res* **276**, 178 (1983).
- S6. S. Chung, X. Li, S. B. Nelson, *Neuron* **34**, 437 (2002).
- S7. D. J. Pinto, J. C. Brumberg, D. J. Simons, *J Neurophysiol* **83**, 1158 (2000).
- S8. S. Temereanca, D. J. Simons, *J Neurophysiol* **89**, 2137 (2003).
- S9. J. M. Alonso, Stoelzel, C.R., Yeh, C.I., Society for Neuroscience Program No. 821.56, Washington, DC 2001.
- S10. L. Gabernet, S. P. Jadhav, D. E. Feldman, M. Carandini, M. Scanziani, *Neuron* **48**, 315 (2005).
- S11. Q. Sun, J. R. Huguenard, D. A. Prince, *J Neurosci* **26**, 1219 (2006).
- S12. J. R. Gibson, M. Beierlein, B. W. Connors, *Nature* **402**, 75 (1999).
- S13. R. Llinas, H. Jahnsen, *Nature* **297**, 406 (1982).
- S14. K. Horikawa, W. E. Armstrong, *J Neurosci Methods* **25**, 1 (1988).
- S15. M. Brecht, A. Roth, B. Sakmann, *J Physiol* **553**, 243 (2003).
- S16. D. Pinault, *J Neurosci Methods* **65**, 113 (1996).
- S17. E. E. Fanselow, M. A. Nicolelis, *J Neurosci* **19**, 7603 (1999).
- S18. D. J. Simons, G. E. Carvell, A. E. Hershey, D. P. Bryant, *Exp Brain Res* **91**, 259 (1992).
- S19. M. E. Lewis, A. Pert, C. B. Pert, M. Herkenham, *J Comp Neurol* **219**, 339 (1983).
- S20. M. Sahin, W. D. Bowen, J. P. Donoghue, *Brain Research* **579**, 135 (1992).
- S21. J. M. Alonso, L. M. Martinez, *Nat Neurosci* **1**, 395 (1998).

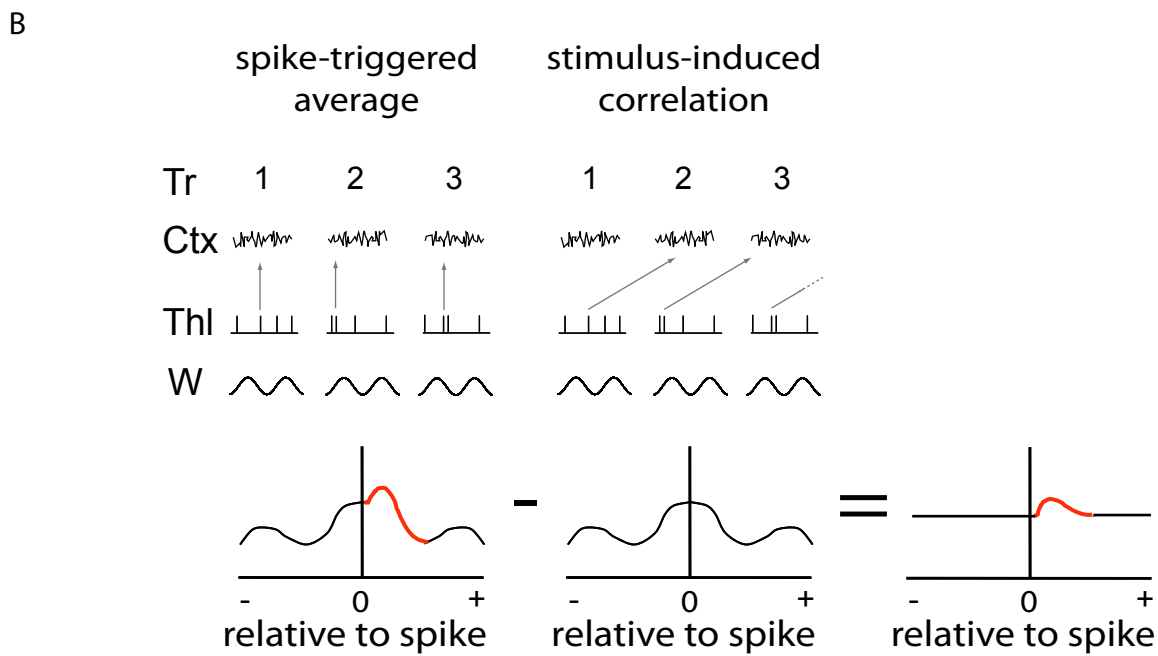
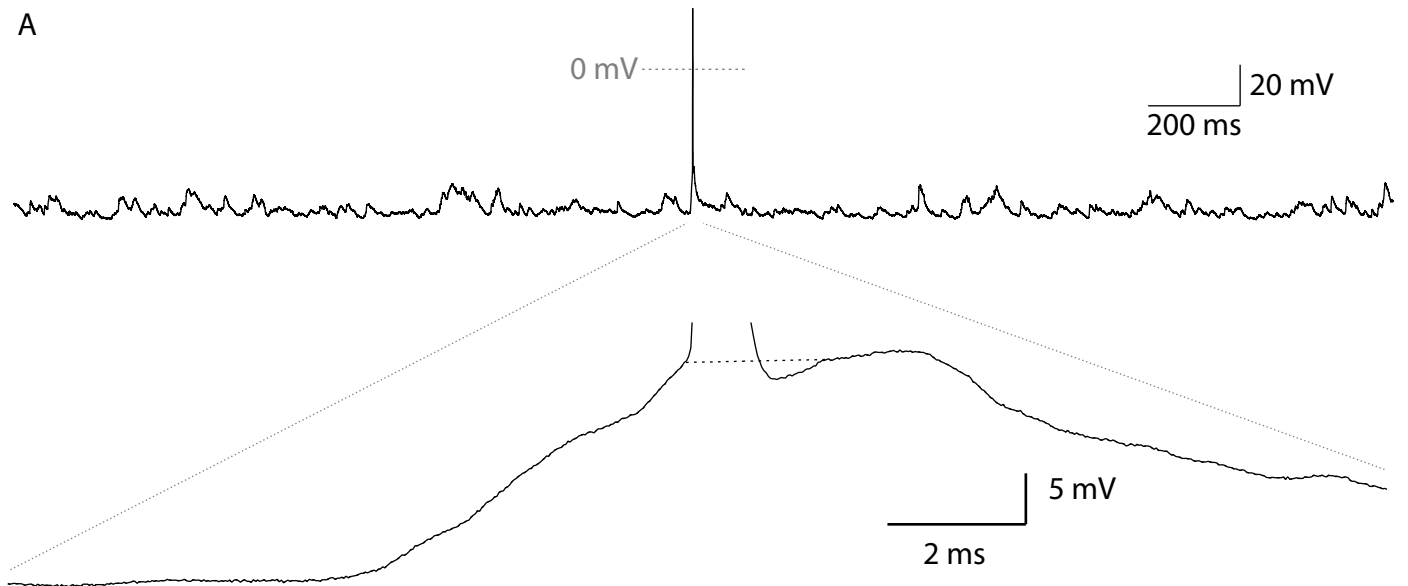
R.M.Bruno & B.Sakmann, Supplementary Figure 1



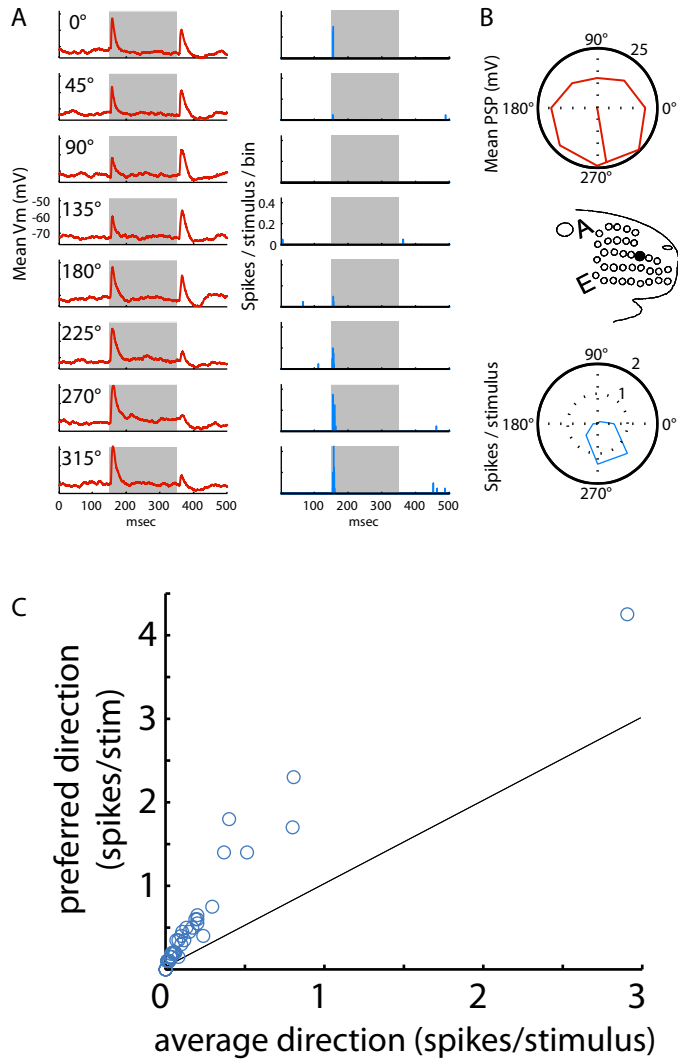
R.M.Bruno & B.Sakmann, Supplementary Figure 2

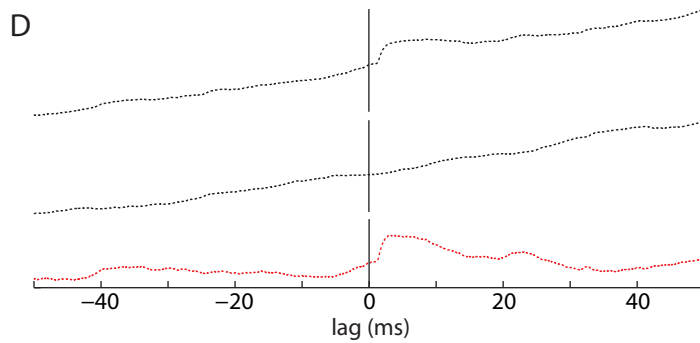
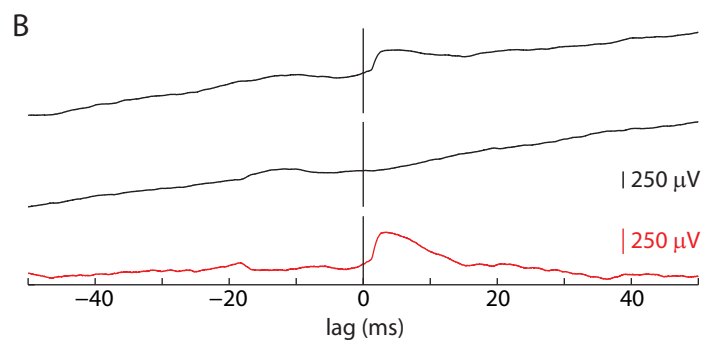
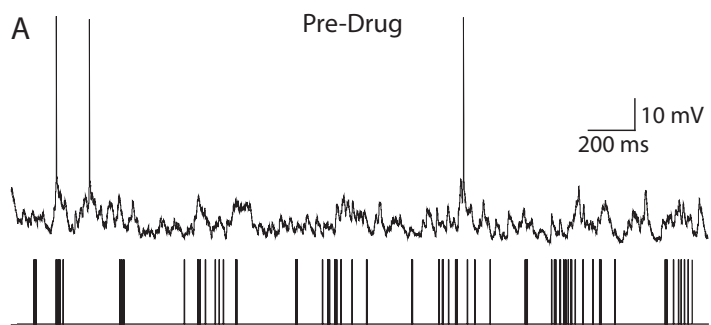


R.M. Bruno & B.Sakmann, Supplementary Figure 3

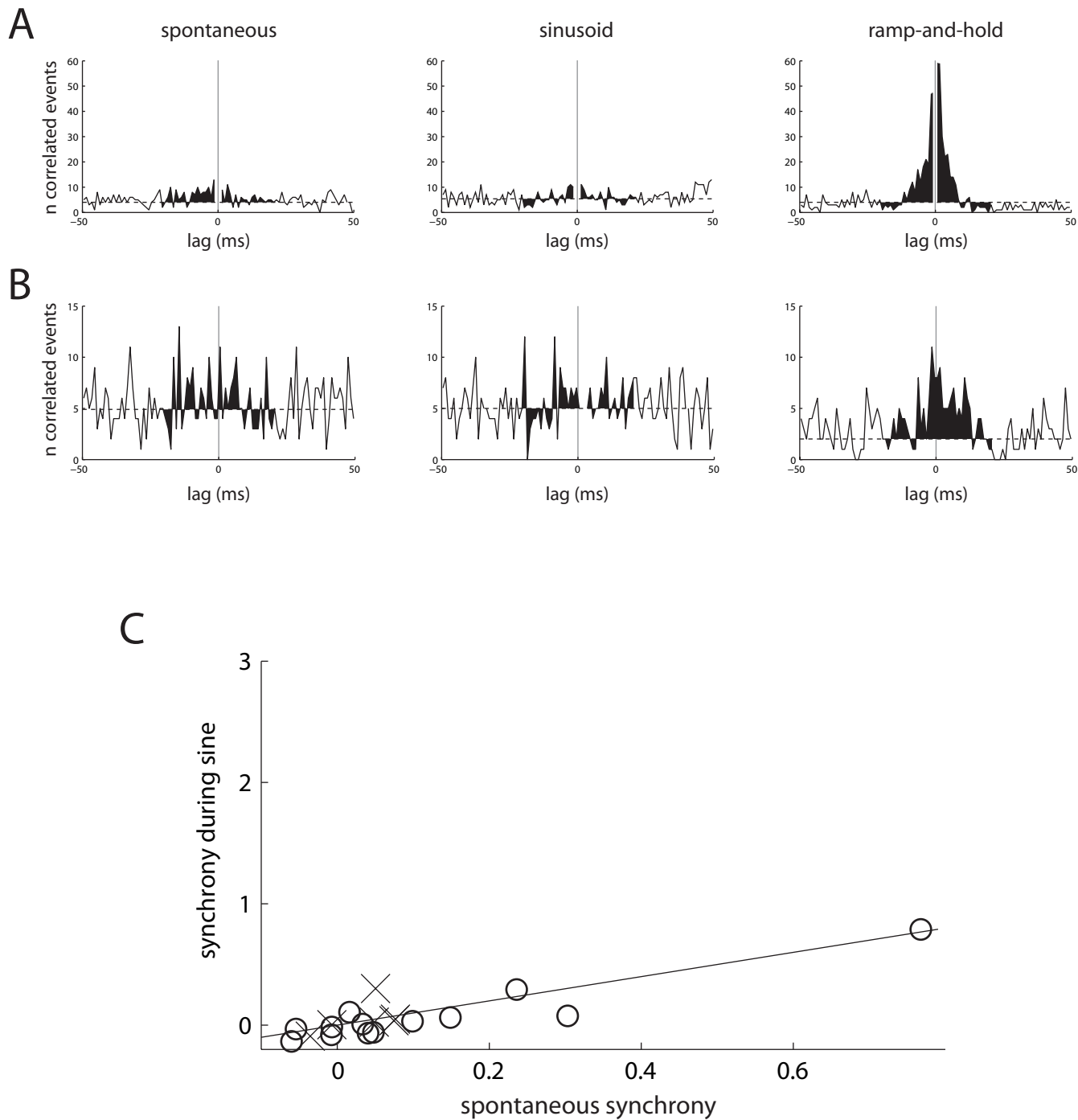


R.M.Bruno & B.Sakmann, Supplementary Figure 4





R.M.Bruno & B.Sakmann, Supplementary Figure 6



R.M.Bruno & B.Sakmann, Supplementary Figure 7

